UCRL- 90577
PREPRINT

Modeling Chemical Kinetic Aspects of Engine Knock

William J. Pitz
Charles K. Westbrook

This paper was prepared for submittal to the Spring Technical Meeting of the Western States Section of The Combustion Institute, Boulder, Colorado, April 2-3, 1984.

March 20, 1984

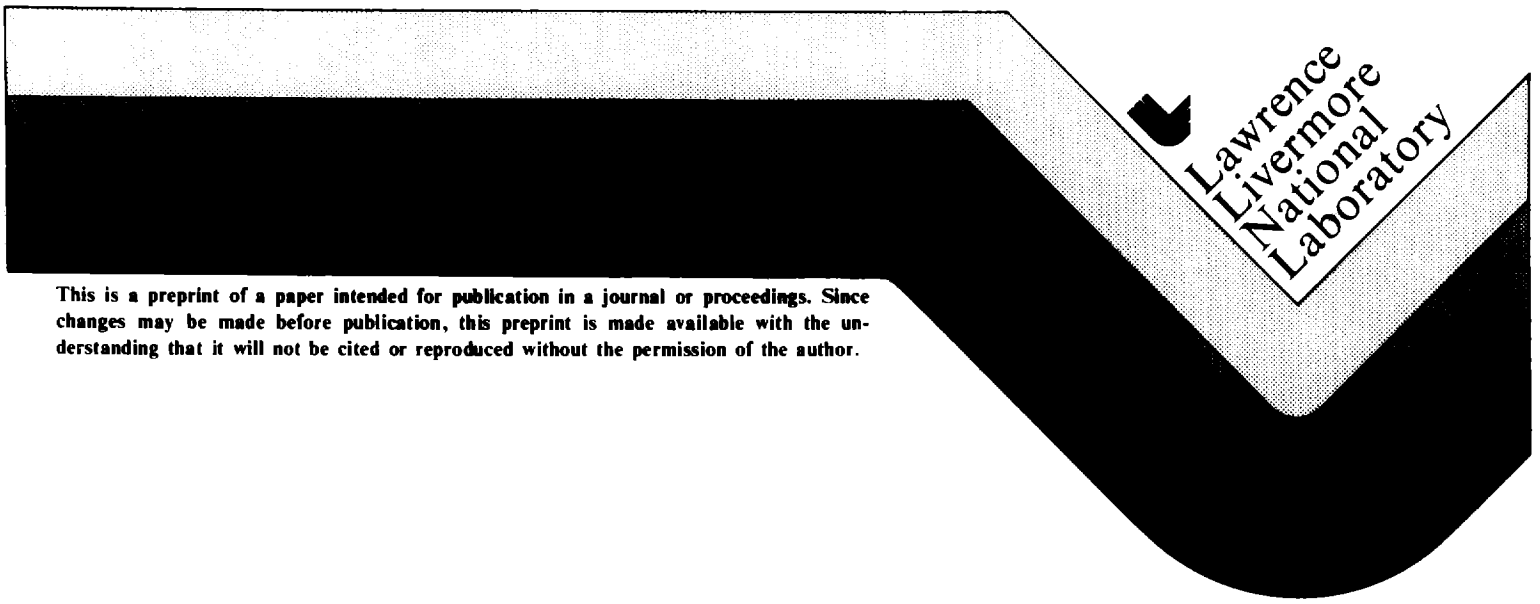

Modeling Chemical Kinetic Aspects of Engine Knock

William J. Pitz and Charles K. Westbrook
Lawrence Livermore National Laboratory
Livermore, California 94550

ABSTRACT

A chemical kinetics oxidation mechanism for n-butane is employed to study hydrocarbon autoignition related to engine knock. A low temperature submechanism has been added to a previously developed high temperature mechanism in order to examine the importance of low temperature reaction paths in autoignition. A series of calculations follows reactions taking place in a sample of end-gas that is subjected to the pressure and temperature history observed in an actual engine. Predicted autoignition times compare very well those experimentally measured by Smith et al. (1984). However, inclusion of a low temperature submechanism did not affect the predicted autoignition times. Controlling chemical reaction paths are identified. Autoignition was found to be particularly sensitive to reactions involving the production and consumption of HO_2.

INTRODUCTION

Increased fuel costs have created a need to improve automotive fuel economy. One can achieve better fuel economy by raising the engine compression ratio, but such increases are limited by the onset of engine

knock. Much interest has developed concerning the chemical and physical processes that control engine knock.

Several modeling studies pertaining to engine knock have recently appeared. Leppard (1983) modeled autoignition in a spark ignition engine. His calculations followed measured temperatures and pressures in an engine and employed the high temperature chemical kinetic mechanism of Westbrook and Dryer (1983) for ethane. No additional reactions were added to address chemical kinetic paths that may become important at low temperatures in the engine cycle. He obtained good agreement (less than 2 crank angle degrees difference) between calculated and measured autoignition times. Halstead et al. (1977) developed a multistep overall kinetic mechanism to study autoignition of hydrocarbons. The mechanism was developed primarily to simulate some of the chemical kinetic paths occurring in the low temperature region relevant to cool flames. Using this global mechanism, Natarajan and Bracco (1983) developed a two-dimensional model to investigate engine knock. Modeling comparisons for a constant volume bomb, rapid compression machine and stirred flow reactor were presented. Carrier et al. (1982) developed an analytical model to study engine knock. They examined the strategy of knock prevention by bulk cooling of the end gas. Maly and Ziegler (1982) employed a thermal model of turbulent flame propagation to investigate processes occurring in engine knock. Dale and Oppenheim (1982) proposed the use of controlled autoignition to reduce automotive emmissions and increase engine efficiency.

A chemical kinetics oxidation mechanism for n-butane has been recently developed (Pitz et al., 1984) and is employed here to study engine knock. N-butane is a more complex fuel than propane whose autoignition characteristics were examined in a previous paper (Pitz and Westbrook, 1983).

N-butane is the simplest hydrocarbon fuel that tends to knock under conditions typically found in spark ignition engines, with a research octane rating of 94 (Obert, 1973), while the next simplest hydrocarbon, propane, has a rating of 112. It also exhibits combustion chemistry characteristics that are similar to much more complex hydrocarbon fuels. For example, it possesses primary and secondary sites for H atom abstraction. In addition, butane occurs in another isomeric form, the branched chain isobutane, which has a much higher Research octane rating of 102 (Obert). Future numerical modeling work will examine the role that branched-chain molecular structure has on knock properties.

During the engine cycle, the end-gas, the last portion of fuel-air mixture in the combustion chamber to be consumed, is subjected to temperatures in the range of 500-800 K for a considerable length of time. Some researchers (Downs et al., 1951) have shown that "cool flame" processes occur at these temperatures and produce peroxides that may act as proknock agents. "Cool flame" kinetic mechanisms have been reviewed extensively by Benson (1982). A central feature of these low temperature mechanisms is the formation of hydroperoxides and their subsequent degenerate branching. This additional chain branching path that is important at low temperatures may lead to accelerated autoignition of the end-gas. In the present work, a low temperature kinetics submechanism has been added to the previously developed high temperature mechanism of n-butane to examine the importance of low temperature reaction paths.

Model calculations which followed reactions taking place in a sample of fuel-air mixture are presented in this work. These calculations simulate the temperature, pressure and species concentration history of a sample of end-gas. The fuel-air mixture was constrained to follow an actual pressure and temperature history of end-gas measured in spark ignition engine.

Pressures and temperatures in a knocking engine have been measured as a function of time under highly reproducible conditions (Smith et al., 1984; Green and Smith, 1984). Schlieren records of the end-gas were also obtained. The model calculations predict the time of autoignition of the end-gas which is then related to the measured time of knock observed by Smith and Green. Calculations were performed with and without the inclusion of cool flame kinetics reactions to assess the importance of low temperature reaction paths.

NUMERICAL MODEL

Numerical calculations were carried out using the HCT computer code (Lund, 1978) which solves the coupled conservation equations of mass, momentum, energy and each chemical species. The detailed reaction mechanism employed in these calculations (Table I) has been developed and validated in a series of previous studies (Pitz et al., 1984; Westbrook and Pitz, 1984). Reverse reaction rates are computed from the forward rates and the appropriate thermodynamic data (JANAF, 1971; Bahn, 1973). This mechanism has been shown to describe the high temperature oxidation ($T > 1000$ K) of n-butane, propane, propene, ethane, ethylene, acetylene, methane, methanol, carbon monoxide and hydrogen over a wide range of experimental conditions.

In order to consider additional kinetic paths which occur below 1000 K, another kinetic submechanism (Table II) was added to the high temperature mechanism. This submechanism contains chemical kinetic steps which pertain to the formation and consumption of hydroperoxides. The rate parameters were estimated on the basis of the work of Benson (1982).

Table I
Fuel oxidation mechanism. Reaction rates in cm^3-mole-sec-kcal units, $k=AT^n\exp(-E_a/RT)$

	Reaction	Forward rate			Reverse rate		
		log A	n	E_a	log A	n	E_a
1.	$H+O_2 \rightarrow O+OH$	16.71	-0.8	16.51	13.12	0	0.68
2.	$H_2+O \rightarrow H+OH$	10.26	1	8.90	9.92	1	6.95
3.	$H_2O+O \rightarrow OH+OH$	13.53	0	18.35	12.50	0	1.10
4.	$H_2O+H \rightarrow H_2+OH$	13.98	0	20.30	13.34	0	5.15
5.	$H_2O_2+OH \rightarrow H_2O+HO_2$	13.00	0	1.80	13.45	0	32.79
6.	$H_2O+M \rightarrow H+OH+M$	16.34	0	105.00	23.15	-2	0.00
7.	$H+O_2+M \rightarrow HO_2+M$	15.22	0	-1.00	15.36	0	45.90
8.	$HO_2+O \rightarrow OH+O_2$	13.70	0	1.00	13.81	0	56.61
9.	$HO_2+H \rightarrow OH+OH$	14.40	0	1.90	13.08	0	40.10
10.	$HO_2+H \rightarrow H_2+O_2$	13.40	0	0.70	13.74	0	57.80
11.	$HO_2+OH \rightarrow H_2O+O_2$	13.70	0	1.00	14.80	0	73.86
12.	$H_2O_2+O_2 \rightarrow HO_2+HO_2$	13.60	0	42.64	13.00	0	1.00
13.	$H_2O_2+M \rightarrow OH+OH+M$	17.08	0	45.50	14.96	0	-5.07
14.	$H_2O_2+H \rightarrow HO_2+H_2$	12.23	0	3.75	11.86	0	18.70
15.	$O+H+M \rightarrow OH+M$	16.00	0	0.00	19.90	-1	103.72
16.	$O_2+M \rightarrow O+O+M$	15.71	0	115.00	15.67	-0.28	0.00
17.	$H_2+M \rightarrow H+H+M$	14.34	0	96.00	15.48	0	0.00
18.	$CO+OH \rightarrow CO_2+H$	7.11	1.3	-0.77	9.15	1.3	21.58
19.	$CO+HO_2 \rightarrow CO_2+OH$	14.18	0	23.65	15.23	0	85.50
20.	$CO+O+M \rightarrow CO_2+M$	15.77	0	4.10	21.74	-1	131.78
21.	$CO_2+O \rightarrow CO+O_2$	12.44	0	43.83	11.50	0	37.60
22.	$HCO+OH \rightarrow CO+H_2O$	14.00	0	0.00	15.45	0	105.15
23.	$HCO+M \rightarrow H+CO+M$	14.16	0	19.00	11.70	1	1.55
24.	$HCO+H \rightarrow CO+H_2$	14.30	0	0.00	15.12	0	90.00
25.	$HCO+O \rightarrow CO+OH$	14.00	0	0.00	14.46	0	87.90
26.	$HCO+HO_2 \rightarrow CH_2O+O_2$	14.00	0	3.00	15.56	0	46.04
27.	$HCO+O_2 \rightarrow CO+HO_2$	12.60	0	7.00	12.95	0	39.29
28.	$CH_2O+M \rightarrow HCO+H+M$	16.52	0	81.00	11.15	1	-11.77
29.	$CH_2O+OH \rightarrow HCO+H_2O$	12.88	0	0.17	12.41	0	29.99
30.	$CH_2O+H \rightarrow HCO+H_2$	14.52	0	10.50	13.42	0	25.17
31.	$CH_2O+O \rightarrow HCO+OH$	13.70	0	4.60	12.24	0	17.17
32.	$CH_2O+HO_2 \rightarrow HCO+H_2O_2$	12.00	0	8.00	11.04	0	6.59
33.	$CH_4+M \rightarrow CH_3+H+M$	17.15	0	88.40	11.45	1	-19.52
34.	$CH_4+H \rightarrow CH_3+H_2$	14.10	0	11.90	12.68	0	11.43
35.	$CH_4+OH \rightarrow CH_3+H_2O$	3.54	3.08	2.00	2.76	3.08	16.68
36.	$CH_4+O \rightarrow CH_3+OH$	6.33	2.21	6.48	4.55	2.21	3.92
37.	$CH_4+HO_2 \rightarrow CH_3+H_2O_2$	13.30	0	18.00	12.02	0	1.45
38.	$CH_3+HO_2 \rightarrow CH_3O+OH$	13.51	0	0.00	10.00	0	0.00
39.	$CH_3+OH \rightarrow CH_2O+H_2$	12.60	0	0.00	14.08	0	71.73
40.	$CH_3+O \rightarrow CH_2O+H$	14.11	0	2.00	15.23	0	71.63
41.	$CH_3+O_2 \rightarrow CH_3O+O$	13.68	0	29.00	14.48	0	0.73
42.	$CH_2O+CH_3 \rightarrow CH_4+HCO$	10.00	0.5	6.00	10.32	0.5	21.14
43.	$CH_3+HCO \rightarrow CH_4+CO$	11.48	0.5	0.00	13.71	0.5	90.47
44.	$CH_3+HO_2 \rightarrow CH_4+O_2$	12.00	0	0.40	13.88	0	58.59
45.	$CH_3O+M \rightarrow CH_2O+H+M$	13.70	0	21.00	9.00	1	-2.56
46.	$CH_3O+O_2 \rightarrow CH_2O+HO_2$	12.00	0	6.00	11.11	0	32.17
47.	$C_2H_6 \rightarrow CH_3+CH_3$	19.35	-1	88.31	12.95	0	0.00
48.	$C_2H_6+CH_3 \rightarrow C_2H_5+CH_4$	-0.26	4	8.28	10.48	0	12.50

Table I (continued)
Fuel oxidation mechanism. Reaction rates in
cm^3-mole-sec-kcal units, $k=AT^n\exp(-E_a/RT)$

	Reaction	Forward rate			Reverse rate		
		log A	n	E_a	log A	n	E_a
49.	$C_2H_6+H \rightarrow C_2H_5+H_2$	2.73	3.5	5.20	2.99	3.5	27.32
50.	$C_2H_6+OH \rightarrow C_2H_5+H_2O$	9.94	1.05	1.81	10.23	1.05	20.94
51.	$C_2H_6+O \rightarrow C_2H_5+OH$	14.04	0	7.85	13.32	0	12.72
52.	$C_2H_5+M \rightarrow C_2H_4+H+M$	15.30	0	30.00	10.62	0	-11.03
53.	$C_2H_5+O_2 \rightarrow C_2H_4+HO_2$	12.00	0	5.00	11.12	0	13.70
54.	$C_2H_4+C_2H_4 \rightarrow C_2H_5+C_2H_3$	14.70	0	64.70	14.17	0	-2.61
55.	$C_2H_4+M \rightarrow C_2H_2+H_2$	16.97	0	77.20	12.66	1	36.52
56.	$C_2H_4+M \rightarrow C_2H_3+H+M$	18.80	0	108.72	17.30	0	0.00
57.	$C_2H_4+O \rightarrow CH_3+HCO$	12.52	0	1.13	11.20	0	31.18
58.	$C_2H_4+O \rightarrow CH_2O+CH_2$	13.40	0	5.00	12.48	0	15.68
59.	$C_2H_4+H \rightarrow C_2H_3+H_2$	7.18	2	6.00	6.24	2	5.11
60.	$C_2H_4+OH \rightarrow C_2H_3+H_2O$	12.68	0	1.23	12.08	0	14.00
61.	$C_2H_4+OH \rightarrow CH_3+CH_2O$	12.30	0	0.96	11.78	0	16.48
62.	$C_2H_3+M \rightarrow C_2H_2+H+M$	14.90	0	31.50	11.09	1	-10.36
63.	$C_2H_3+O_2 \rightarrow C_2H_2+HO_2$	12.00	0	10.00	12.00	0	17.87
64.	$C_2H_2+M \rightarrow C_2H+H+M$	14.00	0	114.00	9.04	1	0.77
65.	$C_2H_2+O_2 \rightarrow HCO+HCO$	12.60	0	28.00	11.00	0	63.65
66.	$C_2H_2+H \rightarrow C_2H+H_2$	14.30	0	19.00	13.62	0	13.21
67.	$C_2H_2+OH \rightarrow C_2H+H_2O$	12.78	0	7.00	12.73	0	16.36
68.	$C_2H_2+OH \rightarrow CH_2CO+H$	11.51	0	0.20	12.50	0	20.87
69.	$C_2H_2+O \rightarrow C_2H+OH$	15.51	-0.6	17.00	14.47	-0.6	0.91
70.	$C_2H_2+O \rightarrow CH_2+CO$	13.83	0	4.00	13.10	0	54.67
71.	$C_2H+O_2 \rightarrow HCO+CO$	13.00	0	7.00	12.93	0	138.40
72.	$C_2H+O \rightarrow CO+CH$	13.70	0	0.00	13.50	0	59.43
73.	$CH_2+O_2 \rightarrow HCO+OH$	14.00	0	3.70	13.61	0	76.58
74.	$CH_2+O \rightarrow CH+OH$	11.28	0.68	25.00	10.77	0.68	25.93
75.	$CH_2+H \rightarrow CH+H_2$	11.43	0.67	25.70	11.28	0.67	28.72
76.	$CH_2+OH \rightarrow CH+H_2O$	11.43	0.67	25.70	11.91	0.67	43.88
77.	$CH+O_2 \rightarrow CO+OH$	11.13	0.67	25.70	11.71	0.67	185.60
78.	$CH+O_2 \rightarrow HCO+O$	13.00	0	0.00	13.13	0	71.95
79.	$CH_3OH+M \rightarrow CH_3+OH+M$	18.48	0	80.00	13.16	1	-10.98
80.	$CH_3OH+OH \rightarrow CH_2OH+H_2O$	12.60	0	2.00	7.27	1.66	25.31
81.	$CH_3OH+O \rightarrow CH_2OH+OH$	12.23	0	2.29	5.90	1.66	8.35
82.	$CH_3OH+H \rightarrow CH_2OH+H_2$	13.48	0	7.00	7.51	1.66	15.16
83.	$CH_3OH+H \rightarrow CH_3+H_2O$	12.72	0	5.34	12.32	0	36.95
84.	$CH_3OH+CH_3 \rightarrow CH_2OH+CH_4$	11.26	0	9.80	6.70	1.66	18.43
85.	$CH_3OH+HO_2 \rightarrow CH_2OH+H_2O_2$	12.80	0	19.36	7.00	1.66	11.44
86.	$CH_2OH+M \rightarrow CH_2O+H+M$	13.40	0	29.00	16.69	-0.66	7.58
87.	$CH_2OH+O_2 \rightarrow CH_2O+HO_2$	12.00	0	6.00	17.94	-1.66	28.32
88.	$C_2H_3+C_2H_4 \rightarrow C_4H_6+H$	12.00	0	7.30	13.00	0	4.70
89.	$C_2H_2+C_2H_2 \rightarrow C_4H_3+H$	13.00	0	45.00	13.18	0	0.00
90.	$C_4H_3+M \rightarrow C_4H_2+H+M$	16.00	0	60.00	11.92	1	2.54
91.	$C_2H_2+C_2H \rightarrow C_4H_2+H$	13.60	0	0.00	14.65	0	0.55
92.	$C_4H_2+M \rightarrow C_4H+H+M$	17.54	0	80.00	12.30	1.0	-16.40
93.	$C_2H_3+H \rightarrow C_2H_2+H_2$	13.30	0	2.50	13.12	0	68.08
94.	$C_3H_8 \rightarrow CH_3+C_2H_5$	16.23	0	84.84	10.18	1	-0.32
95.	$CH_3+C_3H_8 \rightarrow CH_4+iC_3H_7$	15.04	0	25.14	15.64	0	32.12
96.	$CH_3+C_3H_8 \rightarrow CH_4+nC_3H_7$	15.04	0	25.14	15.64	0	32.12

Table I (continued)
Fuel oxidation mechanism. Reaction rates in
cm^3-mole-sec-kcal units, $k=AT^n\exp(-E_a/RT)$

	Reaction	Forward rate			Reverse rate		
		log A	n	E_a	log A	n	E_a
97.	$H+C_3H_8 \rightarrow H_2+iC_3H_7$	6.94	2	5.00	12.89	0	15.87
98.	$H+C_3H_8 \rightarrow H_2+nC_3H_7$	7.75	2	7.70	12.96	0	14.46
99.	$iC_3H_7 \rightarrow H+C_3H_6$	13.80	0	36.90	13.00	0	1.50
100.	$iC_3H_7 \rightarrow CH_3+C_2H_4$	10.30	0	29.50	4.66	1	4.29
101.	$nC_3H_7 \rightarrow CH_3+C_2H_4$	13.98	0	31.00	8.34	1	5.79
102.	$nC_3H_7 \rightarrow H+C_3H_6$	14.10	0	37.00	13.00	0	1.50
103.	$iC_3H_7+C_3H_8 \rightarrow nC_3H_7+C_3H_8$	10.48	0	12.90	10.48	0	12.90
104.	$C_2H_3+C_3H_8 \rightarrow C_2H_4+iC_3H_7$	11.00	0	10.40	11.12	0	17.80
105.	$C_2H_3+C_3H_8 \rightarrow C_2H_4+nC_3H_7$	11.00	0	10.40	11.12	0	17.80
106.	$C_2H_5+C_3H_8 \rightarrow C_2H_6+iC_3H_7$	11.00	0	10.40	10.56	0	9.93
107.	$C_2H_5+C_3H_8 \rightarrow C_2H_6+nC_3H_7$	11.00	0	10.40	10.56	0	9.93
108.	$C_3H_8+O \rightarrow iC_3H_7+OH$	13.45	0	5.20	12.27	0	7.41
109.	$C_3H_8+O \rightarrow nC_3H_7+OH$	14.05	0	7.85	12.88	0	9.61
110.	$C_3H_8+OH \rightarrow iC_3H_7+H_2O$	8.68	1.4	0.85	8.93	1.25	22.37
111	$C_3H_8+OH \rightarrow nC_3H_7+H_2O$	8.76	1.4	0.85	9.01	1.25	22.37
112.	$C_3H_8+HO_2 \rightarrow iC_3H_7+H_2O_2$	12.53	0	17.00	11.84	0	7.43
113.	$C_3H_8+HO_2 \rightarrow nC_3H_7+H_2O_2$	13.05	0	19.40	12.37	0	9.83
114.	$C_3H_6+O \rightarrow C_2H_4+CH_2O$	13.77	0	5.00	13.76	0	86.67
115.	$iC_3H_7+O_2 \rightarrow C_3H_6+HO_2$	12.00	0	5.00	11.30	0	17.48
116.	$nC_3H_7+O_2 \rightarrow C_3H_6+HO_2$	12.00	0	5.00	11.30	0	17.48
117.	$C_3H_8+O_2 \rightarrow iC_3H_7+HO_2$	13.60	0	47.50	12.31	0	0.00
118.	$C_3H_8+O_2 \rightarrow nC_3H_7+HO_2$	13.60	0	47.50	12.31	0	0.00
119.	$C_3H_6+OH \rightarrow C_2H_5+CH_2O$	12.90	0	0.00	13.66	0	17.35
120.	$C_3H_6+O \rightarrow C_2H_5+HCO$	12.55	0	0.00	11.85	0	29.92
121.	$C_3H_6+OH \rightarrow CH_3+CH_3CHO$	11.54	0	0.00	11.44	0	20.40
122.	$C_3H_6+O \rightarrow CH_3+CH_3CO$	13.07	0	0.60	12.25	0	38.37
123.	$CH_3CHO+H \rightarrow CH_3CO+H_2$	13.60	0	4.20	13.25	0	23.67
124.	$CH_3CHO+OH \rightarrow CH_3CO+H_2O$	13.00	0	0.00	13.28	0	36.62
125.	$CH_3CHO+O \rightarrow CH_3CO+OH$	12.70	0	1.79	12.00	0	19.16
126.	$CH_3CHO+CH_3 \rightarrow CH_3CO+CH_4$	12.23	0	8.43	13.48	0	28.00
127.	$CH_3CHO+HO_2 \rightarrow CH_3CO+H_2O_2$	12.23	0	10.70	12.00	0	14.10
128.	$CH_3CHO \rightarrow CH_3+HCO$	15.85	0	81.78	9.58	1	0.00
129.	$CH_3CHO+O_2 \rightarrow CH_3CO+HO_2$	13.30	0.5	42.20	7.00	0.5	4.00
130.	$CH_3CO \rightarrow CH_3+CO$	13.48	0	17.24	11.20	0	5.97
131.	$C_3H_6+H \rightarrow C_3H_5+H_2$	12.70	0	1.50	12.18	0	17.70
132.	$C_3H_6+CH_3 \rightarrow C_3H_5+CH_4$	10.95	0	8.50	11.87	0	25.18
133.	$C_3H_6+C_2H_5 \rightarrow C_3H_5+C_2H_6$	11.00	0	9.20	5.00	0	56.77
134.	$C_3H_6+OH \rightarrow C_3H_5+H_2O$	12.60	0	0.00	7.18	0	69.69
135.	$C_3H_8+C_3H_5 \rightarrow iC_3H_7+C_3H_6$	11.60	0	16.20	11.30	0	6.50
136.	$C_3H_8+C_3H_5 \rightarrow iC_3H_7+C_3H_6$	11.60	0	16.20	11.30	0	6.50
137.	$C_3H_5 \rightarrow C_3H_4+H$	13.60	0	70.00	8.00	1	0.00
138.	$C_3H_5+O_2 \rightarrow C_3H_4+HO_2$	11.78	0	10.00	11.08	0	10.00
139.	$1C_4H_8 \rightarrow C_3H_5+CH_3$	19.18	-1	73.40	13.13	0	0.00
140.	$1C_4H_8 \rightarrow C_2H_3+C_2H_5$	19.00	-1	96.77	12.95	0	0.00
141.	$1C_4H_8+O \rightarrow CH_3CHO+C_2H_4$	13.11	0	0.85	12.32	0	85.10
142.	$1C_4H_8+O \rightarrow CH_3CO+C_2H_5$	13.11	0	0.85	12.37	0	38.15
143.	$1C_4H_8+OH \rightarrow CH_3CHO+C_2H_5$	13.00	0	0.00	12.97	0	19.93
144.	$1C_4H_8+OH \rightarrow CH_3CO+C_2H_6$	13.00	0	0.00	12.99	0	32.43

Table I (continued)
Fuel oxidation mechanism. Reaction rates in
cm^3-mole-sec-kcal units, $k=AT^n\exp(-E_a/RT)$

	Reaction	Forward rate log A	n	E_a	Reverse rate log A	n	E_a
145.	$C_3H_4+O \rightarrow CH_2O+C_2H_2$	12.00	0	0.00	12.03	0	81.73
146.	$C_3H_4+O \rightarrow HCO+C_2H_3$	12.00	0	0.00	10.47	0	30.82
147.	$C_3H_4+OH \rightarrow CH_2O+C_2H_3$	12.00	0	0.00	11.93	0	18.25
148.	$C_3H_4+OH \rightarrow HCO+C_2H_4$	12.00	0	0.00	11.77	0	33.81
149.	$C_3H_6 \rightarrow C_3H_5+H$	13.00	0	78.00	11.00	0	0.00
150.	$C_2H_2+O \rightarrow HCCO+H$	4.55	2.7	1.39	2.70	2.7	12.79
151.	$CH_2CO+H \rightarrow CH_3+CO$	13.04	0	3.40	12.38	0	40.20
152.	$CH_2CO+O \rightarrow HCO+HCO$	13.00	0	2.40	11.54	0	33.50
153.	$CH_2CO+OH \rightarrow CH_2O+HCO$	13.45	0	0.00	13.44	0	18.50
154.	$CH_2CO+M \rightarrow CH_2+CO+M$	16.30	0	60.00	10.66	0	0.00
155.	$CH_2CO+O \rightarrow HCCO+OH$	13.70	0	8.00	10.86	0	8.00
156.	$CH_2CO+OH \rightarrow HCCO+H_2O$	12.88	0	3.00	11.03	0	11.00
157.	$CH_2CO+H \rightarrow HCCO+H_2$	13.88	0	8.00	11.39	0	8.00
158.	$HCCO+OH \rightarrow HCO+HCO$	13.00	0	0.00	13.68	0	40.36
159.	$HCCO+H \rightarrow CH_2+CO$	13.70	0	0.00	13.82	0	39.26
160.	$HCCO+O \rightarrow HCO+CO$	13.53	0	2.00	13.92	0	128.26
161.	$C_3H_6 \rightarrow C_2H_3+CH_3$	15.80	0	85.80	10.00	1	0.00
162.	$C_3H_5+H \rightarrow C_3H_4+H_2$	13.00	0	0.00	13.00	0	40.00
163.	$C_3H_5+CH_3 \rightarrow C_3H_4+CH_4$	12.00	0	0.00	13.00	0	40.00
164.	$C_2H_6+O_2 \rightarrow C_2H_5+HO_2$	13.00	0	51.00	12.00	0	0.00
165.	$C_2H_6+HO_2 \rightarrow C_2H_5+H_2O_2$	11.48	0	11.50	11.23	0	2.39
166.	$CH_3+C_2H_3 \rightarrow CH_4+C_2H_2$	12.00	0	0.00	13.88	0	66.05
167.	$CH_3+C_2H_5 \rightarrow CH_4+C_2H_4$	11.90	0	0.00	12.91	0	66.89
168.	$C_2H_5+C_3H_5 \rightarrow C_3H_6+C_2H_4$	12.10	0	0.00	10.00	0	50.00
169.	$C_2H_5+C_2H_5 \rightarrow C_2H_6+C_2H_4$	12.60	0	0.00	12.60	0	60.00
170.	$CH_3OH+CH_2O \rightarrow CH_3O+CH_3O$	12.19	0	79.57	13.48	0	0.00
171.	$CH_2O+CH_3O \rightarrow CH_3OH+HCO$	10.43	0	3.00	8.47	0	13.37
172.	$CH_4+CH_3O \rightarrow CH_3OH+CH_3$	11.30	0	7.00	9.02	0	2.22
173.	$C_2H_6+CH_3O \rightarrow CH_3OH+C_2H_5$	11.48	0	7.00	10.23	0	9.67
174.	$C_3H_8+CH_3O \rightarrow CH_3OH+iC_3H_7$	11.48	0	7.00	10.23	0	9.67
175.	$C_3H_8+CH_3O \rightarrow CH_3OH+nC_3H_7$	11.48	0	7.00	10.23	0	9.67
176.	$C_4H_{10} \rightarrow C_2H_5+C_2H_5$	16.30	0	81.30	10.60	1	-2.94
177.	$C_4H_{10} \rightarrow nC_3H_7+CH_3$	17.00	0	85.40	10.51	1	-2.49
178.	$C_4H_{10}+O_2 \rightarrow pC_4H_9+HO_2$	13.40	0	49.00	12.40	0	-2.20
179.	$C_4H_{10}+O_2 \rightarrow sC_4H_9+HO_2$	13.60	0	47.60	12.61	0	-3.62
180.	$C_4H_{10}+H \rightarrow pC_4H_9+H_2$	7.75	2	7.70	12.96	0	14.46
181.	$C_4H_{10}+H \rightarrow sC_4H_9+H_2$	7.24	2	5.00	13.19	0	15.87
182.	$C_4H_{10}+OH \rightarrow pC_4H_9+H_2O$	9.94	1.05	1.81	10.17	1.05	23.33
183.	$C_4H_{10}+OH \rightarrow sC_4H_9+H_2O$	9.41	1.25	0.70	9.66	1.25	22.22
184.	$C_4H_{10}+O \rightarrow pC_4H_9+OH$	14.05	0	7.85	13.17	0	12.24
185.	$C_4H_{10}+O \rightarrow sC_4H_9+OH$	13.75	0	5.20	12.87	0	9.59
186.	$C_4H_{10}+CH_3 \rightarrow pC_4H_9+CH_4$	12.11	0	11.60	13.00	0	18.56
187.	$C_4H_{10}+CH_3 \rightarrow sC_4H_9+CH_4$	11.90	0	9.50	12.80	0	16.46
188.	$C_4H_{10}+C_2H_3 \rightarrow pC_4H_9+C_2H_4$	12.00	0	18.00	12.41	0	25.38
189.	$C_4H_{10}+C_2H_3 \rightarrow sC_4H_9+C_2H_4$	11.90	0	16.80	12.31	0	24.18
190.	$C_4H_{10}+C_2H_5 \rightarrow pC_4H_9+C_2H_6$	11.00	0	13.40	10.85	0	12.92
191.	$C_4H_{10}+C_2H_5 \rightarrow sC_4H_9+C_2H_6$	11.00	0	10.40	10.85	0	9.92
192.	$C_4H_{10}+C_3H_5 \rightarrow pC_4H_9+C_3H_6$	11.60	0	18.80	12.00	0	20.00

Table I (continued)
Fuel oxidation mechanism. Reaction rates in
cm^3-mole-sec-kcal units, $k=AT^n\exp(-E_a/RT)$

	Reaction	Forward rate			Reverse rate		
		log A	n	E_a	log A	n	E_a
193.	$C_4H_{10}+C_3H_5 \rightarrow sC_4H_9+C_3H_6$	11.90	0	16.80	12.00	0	20.00
194.	$C_4H_{10}+HO_2 \rightarrow pC_4H_9+H_2O_2$	13.05	0	19.40	12.66	0	0.00
195.	$C_4H_{10}+HO_2 \rightarrow sC_4H_9+H_2O_2$	12.83	0	17.00	12.44	0	0.00
196.	$C_4H_{10}+CH_3O \rightarrow pC_4H_9+CH_3OH$	11.48	0	7.00	10.09	0	9.18
197.	$C_4H_{10}+CH_3O \rightarrow sC_4H_9+CH_3OH$	11.78	0	7.00	10.39	0	9.18
198.	$pC_4H_9 \rightarrow C_2H_5+C_2H_4$	13.40	0	28.80	11.48	0	8.00
199.	$pC_4H_9 \rightarrow {}_1C_4H_8+H$	13.10	0	38.60	13.00	0	1.50
200.	$pC_4H_9+O_2 \rightarrow {}_1C_4H_8+HO_2$	12.00	0	2.00	11.29	0	15.85
201.	$sC_4H_9 \rightarrow {}_2C_4H_8+H$	12.70	0	37.90	13.00	0	1.50
202.	$sC_4H_9 \rightarrow {}_1C_4H_8+H$	13.30	0	40.40	13.00	0	1.50
203.	$sC_4H_9 \rightarrow C_3H_6+CH_3$	14.30	0	33.20	11.50	0	7.40
204.	$sC_4H_9+O_2 \rightarrow {}_1C_4H_8+HO_2$	12.00	0	4.50	11.29	0	18.35
205.	$sC_4H_9+O_2 \rightarrow {}_2C_4H_8+HO_2$	12.30	0	4.25	11.59	0	18.10
206.	${}_1C_4H_8 \rightarrow C_4H_7+H$	18.61	-1	97.35	13.70	0	0.00
207.	${}_2C_4H_8 \rightarrow C_4H_7+H$	18.61	-1	97.35	13.70	0	0.00
208.	${}_1C_4H_8+H \rightarrow C_4H_7+H_2$	13.70	0	3.90	10.00	0	13.99
209.	${}_2C_4H_8+H \rightarrow C_4H_7+H_2$	13.70	0	3.80	10.00	0	13.89
210.	${}_1C_4H_8+OH \rightarrow C_4H_7+H_2O$	12.68	0	1.23	12.68	0	26.47
211.	${}_2C_4H_8+OH \rightarrow C_4H_7+H_2O$	12.68	0	1.23	12.68	0	26.47
212.	${}_1C_4H_8+CH_3 \rightarrow C_4H_7+CH_4$	11.00	0	7.30	11.78	0	17.86
213.	${}_2C_4H_8+CH_3 \rightarrow C_4H_7+CH_4$	11.00	0	8.20	11.78	0	18.76
214.	${}_1C_4H_8+O \rightarrow C_3H_6+CH_2O$	12.70	0	0.00	12.14	0	81.33
215.	${}_2C_4H_8+O \rightarrow iC_3H_7+HCO$	12.78	0	0.00	11.35	0	25.81
216.	${}_2C_4H_8+O \rightarrow C_2H_4+CH_3CHO$	12.00	0	0.00	11.20	0	84.25
217.	${}_1C_4H_8+OH \rightarrow iC_3H_7+CH_2O$	13.26	0	0.00	13.29	0	13.23
218.	${}_2C_4H_8+OH \rightarrow C_2H_5+CH_3CHO$	13.41	0	0.00	13.39	0	19.93
219.	$C_4H_7+M \rightarrow C_4H_6+H+M$	14.08	0	49.30	13.60	0	1.30
220.	$C_4H_7+M \rightarrow C_2H_4+C_2H_3+M$	11.00	0	37.00	4.96	1	-3.44
221.	$C_4H_7+O_2 \rightarrow C_4H_6+HO_2$	11.00	0	0.00	10.06	0	-0.90
222.	$C_4H_7+H \rightarrow C_4H_6+H_2$	13.50	0	0.00	13.03	0	56.81
223.	$C_4H_7+C_2H_3 \rightarrow C_4H_6+C_2H_4$	12.60	0	0.00	13.06	0	57.71
224.	$C_4H_7+C_2H_5 \rightarrow C_4H_6+C_2H_6$	12.60	0	0.00	12.51	0	49.84
225.	$C_4H_7+C_2H_5 \rightarrow {}_1C_4H_8+C_2H_4$	11.70	0	0.00	11.93	0	56.33
226.	$C_4H_7+C_2H_5 \rightarrow {}_2C_4H_8+C_2H_4$	11.70	0	0.00	11.93	0	56.33
227.	$C_4H_7+C_3H_5 \rightarrow C_4H_6+C_3H_6$	12.80	0	0.00	10.00	0	50.00
228.	$C_4H_6 \rightarrow C_2H_3+C_2H_3$	19.60	-1	98.15	13.10	0	0.00
229.	$C_4H_6+OH \rightarrow C_2H_5+CH_2CO$	12.00	0	0.00	12.57	0	30.02
230.	$C_4H_6+OH \rightarrow C_3H_5+CH_2O$	12.00	0	0.00	6.54	0	71.06
231.	$C_4H_6+OH \rightarrow C_2H_3+CH_3CHO$	12.00	0	0.00	11.74	0	18.55
232.	$C_4H_6+O \rightarrow C_2H_4+CH_2CO$	12.00	0	0.00	11.80	0	94.34
233.	$C_4H_6+O \rightarrow C_3H_4+CH_2O$	12.00	0	0.00	12.03	0	79.05
234.	$C_5H_{10} \rightarrow CH_3+C_4H_7$	19.00	-1	81.55	13.40	0	0.00
235.	$C_5H_{10}+O \rightarrow {}_1C_4H_8+CH_2O$	12.00	0	0.00	11.41	0	85.43
236.	$C_5H_{10}+O \rightarrow C_3H_6+CH_3CHO$	12.00	0	0.00	10.62	0	88.01
237.	$C_5H_{10}+OH \rightarrow pC_4H_9+CH_2O$	12.00	0	0.00	12.01	0	50.00
238.	$C_5H_{10}+OH \rightarrow nC_3H_7+CH_3CHO$	12.00	0	0.00	11.22	0	50.00

Table II

Low temperature kinetics submechanism. Reaction rates in cm^3-mole-sec-kcal units, $k=AT^n\exp(-E_a/RT)$

	Reaction		Forward rate			Reverse rate			
			log A	n	E_a	log A	n	E_a	Ref.
1.	$R+O_2$	RO_2	12.0	0	0.0	17.8	-1	31.2	a
2.	R_aH(primary)$+RO_2$	R_a+ROOH	10.7	0	16.5	9.6	0	8.0	b
3.	R_aH(sec.)$+RO_2$	R_a+ROOH	11.2	0	16.5	10.1	0	8.0	a
4.	RO_2+CH_2O	ROOH+HCO	11.1	0	9.0	10.4	0	10.1	a
5.	RO_2+CH_3CHO	$ROOH+CH_3CHO$	11.1	0	9.0	10.4	0	10.1	a
6.	RO_2+HO_2	$ROOH+O_2$	12.0	0	0.0	12.5	0	39.0	a
7.	ROOH	RO+OH	15.6	0	43.0	16.8	1	33.9	a
8.	C_2H_5O	CH_3+CH_2O	13.2	0	17.8	5.3	1	9.8	c
9.	nC_3H_7O	$C_2H_5+CH_2O$	13.2	0	17.8	5.3	1	9.8	b
10.	iC_3H_7O	CH_3+CH_3CHO	13.2	0	14.8	5.3	1	9.8	c
11.	pC_4H_9O	$nC_3H_7+CH_2O$	13.2	0	17.8	5.3	1	9.8	b
12.	sC_4H_9O	$C_2H_5+CH_3CHO$	13.2	0	14.8	5.3	1	9.8	b
13.	$C_2H_5O+O_2$	CH_3CHO+H_2O	12.0	0	6.0	11.1	0	32.2	b

R = CH_3, C_2H_5, nC_3H_7, iC_3H_7, pC_4H_9, sC_4H_9

R_a = pC_4H_9, sC_4H_9, nC_3H_7, iC_3H_7

a Benson (1982)

b Estimated by authors

c Martinez et al. (1974)

RESULTS

A series of calculations followed reactions taking place in a sample of end-gas. The calculations used temperature and pressure histories experimentally measured in a spark ignition engine (Smith et al., 1984; Green and Smith, 1984). The engine was fueled by n-butane and operated in a highly reproducible, knocking condition. The objective of these calculations was to simulate the conditions seen by the end-gas in an actual engine and predict the time of autoignition. The calculation was started at 22 degrees (6 ms) before top dead center (BTDC) which is the time of the first temperature data point. In the calculation, a stoichiometric mixture of n-butane-air was constrained to follow the temporal temperature and pressure history observed in the experimental engine. The measured pressures shown in Fig. 1a (Green and Smith, 1984) were followed for the entire calculation. The measured temperatures where followed until the time just prior to the experimental knock point. This is the point just before the measured temperature rises sharply at knock. After this time, the model mixture was allowed to achieve its own temperature which depended on chemical reaction heat release and compressional heating. Eventually, the calculated temperature rose sharply, indicating that autoignition had occurred.

The temperature, pressure, and fuel concentration histories are shown in Fig. 1a and 1b. A chemical kinetics mechanism consisting of both Tables I and II was employed in the calculation. The autoignition time is predicted to be 3.6 ms ATDC which compares well with the measured time of 3.2 ms.

This case was then recalculated with the low temperature mechanism absent. The predicted autoignition time of 3.2 ms was unchanged from the above result. Consequently, the low temperature mechanism had no observable

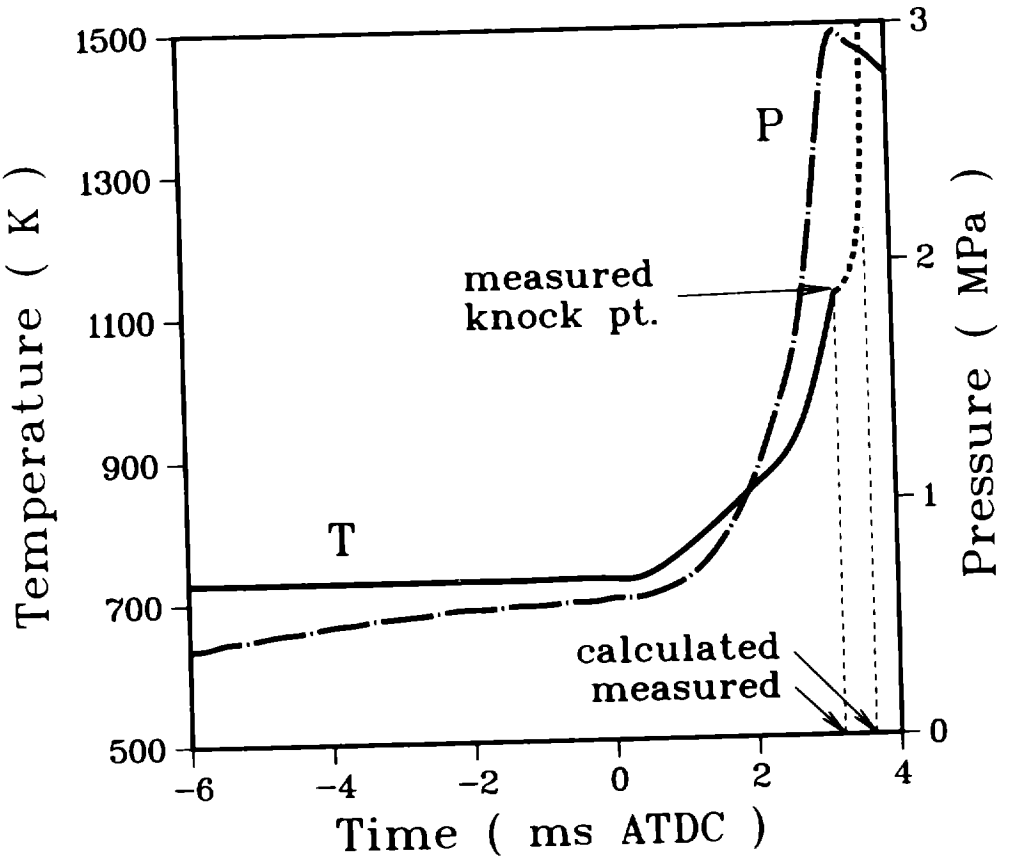

Figure 1a. Pressure and temperature histories of the end-gas. Comparison between calculation and experiment (Green and Smith, 1984). Time is relative to TDC. (Engine speed, 600 rpm; manifold temperature, 423 K; manifold pressure, 1.5 atm absolute; ——— measured temperature; – – – – calculated temperature; — . — measured pressure)

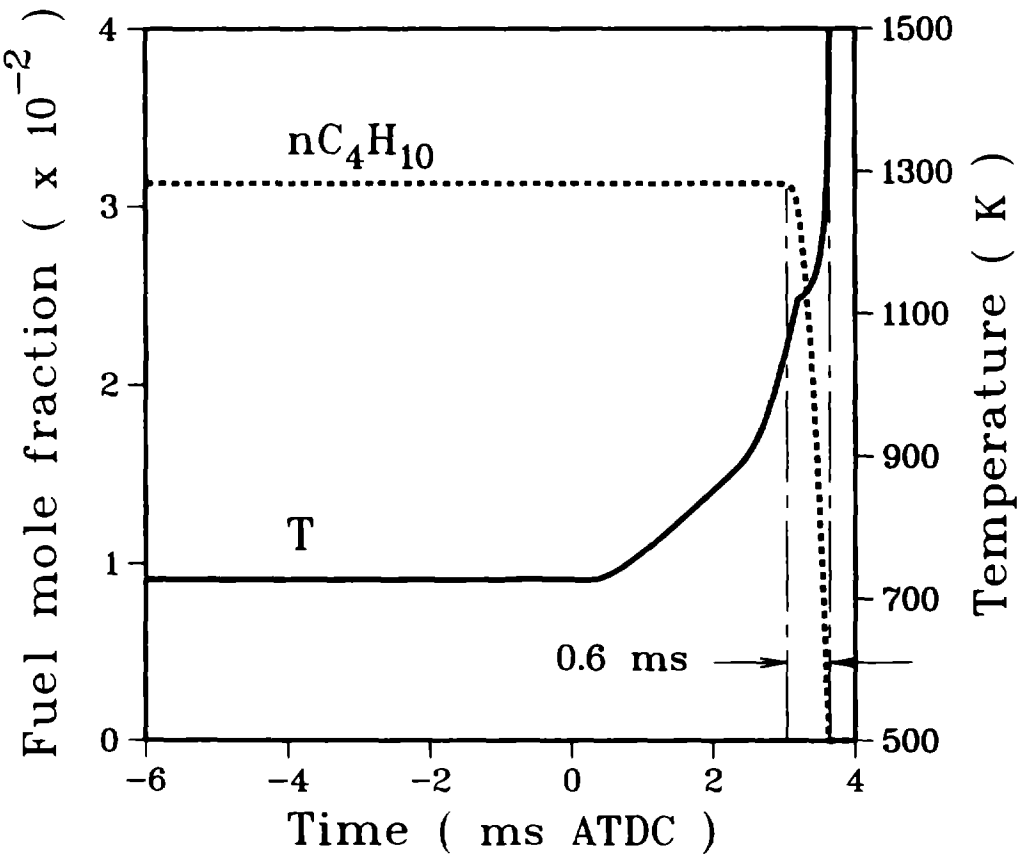

Figure 1b. Calculated fuel concentration and calculated temperature in end-gas.

effect on the calculated autoignition time. This result can be explained by examining the fuel disappearance rate during the calculation. For most of the calculation, the fuel-air mixture resides below 800 K (Fig. 1a) where the characteristic time for fuel disappearance is about 270 ms (Fig. 3, to be discussed later). This characteristic time is about 40 times longer than the time available ($\sim$7 ms, Fig. 1a) for reactions to take place. Therefore, the fuel consumption rate is very small during the low temperature portions of the calculation. As reported in Fig. 1b, the fuel concentration only begins to drop off at about 1050 K when the fuel consumption rate becomes significant. The fuel is being consumed almost entirely at temperatures above 1050 K and in a relatively short time period of 0.6 ms (Fig. 1b).

In one set of calculations, the reactions in a sample of fuel-air mixture were traced from a much earlier time in the engine cycle. In the Sandia engine (Smith et al., 1984), the end-gas spends a considerable time at temperatures in the range of 420-700 K where low temperature reaction paths may be important. The calculation was started at 180° BTDC to assess whether the low temperature reactions in Table II contribute to autoignition. In this case (Fig. 2), the temperatures calculated were a result of initial conditions of 550 K and 0.9 atm at 180° BTDC, experimentally measured pressures from Green and Smith (1984), and an assumption of an adiabatic compression. The initial pressure of 0.9 atm was estimated using a volumetric efficiency of 0.6 and a manifold pressure of 1.5 atm. Cases were run with and without the inclusion of a low temperature reaction scheme (Table II). However, the low temperature submechanism again did not have any observable influence on the autoignition time. Additionally, a series of sensitivity runs were performed where the reaction rates of Table II were varied by an order of magnitude; but the autoignition time remained unchanged. The sample of fuel-air mixture

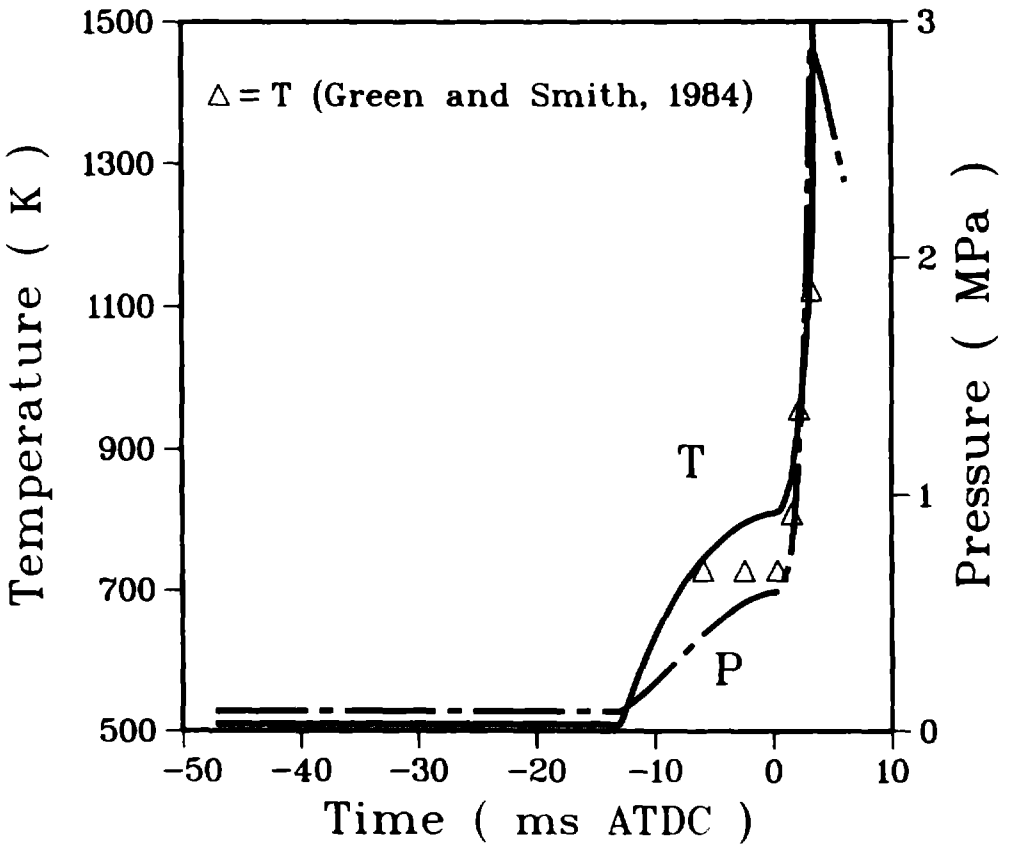

Figure 2. Predicted temperature of end-gas when calculation was started at 180° (47.2 ms) before TDC. (—— - —— experimentally measured pressures used in calculation; Δ experimental temperatures. Both from Green and Smith, 1984).

spends an insufficient amount of time at these lower temperatures for the reaction paths considered to have any effect.

Constant volume calculations showed that the low temperature paths of Table II are important only at very long residence times. In these adiabatic calculations, autoignition of a stoichiometric, n-butane-air mixture at constant volume and an initial pressure of 30 atm was examined. The initial pressure was chosen to be approximately the pressure the end-gas experiences just prior to knock. During the induction period of the calculation, the mixture remains at a nearly constant temperature for a relatively long period of time. Just before autoignition, the temperature rises very steeply which indicates ignition has taken place. Characteristic autoignition times for different initial temperatures are given in Fig. 3. Two series of calculations were made: one series employed the high temperature reaction mechanism only (Table I), and the other series included both the high and low temperature mechanisms (Tables I and II). For $T < 600$ K, the characteristic autoignition time is affected by the low temperature paths; however, the autoignition times in this temperature regime are very long and are 3 to 4 orders of magnitude greater than the time available for autoignition in a spark ignition engine.

The calculations carried out in this study are simplified treatments and neglect some complex processes that occur in the end-gas of a real engine. Multidimensional flows and turbulence affect the onset and severity of knock. Turbulent temperature fluctuations cause some fluid elements in the end gas to autoignite before others. Various autoignition sites interact with each other in a multidimensional geometry. To consider this additional behavior, more complex modeling may need to be performed.

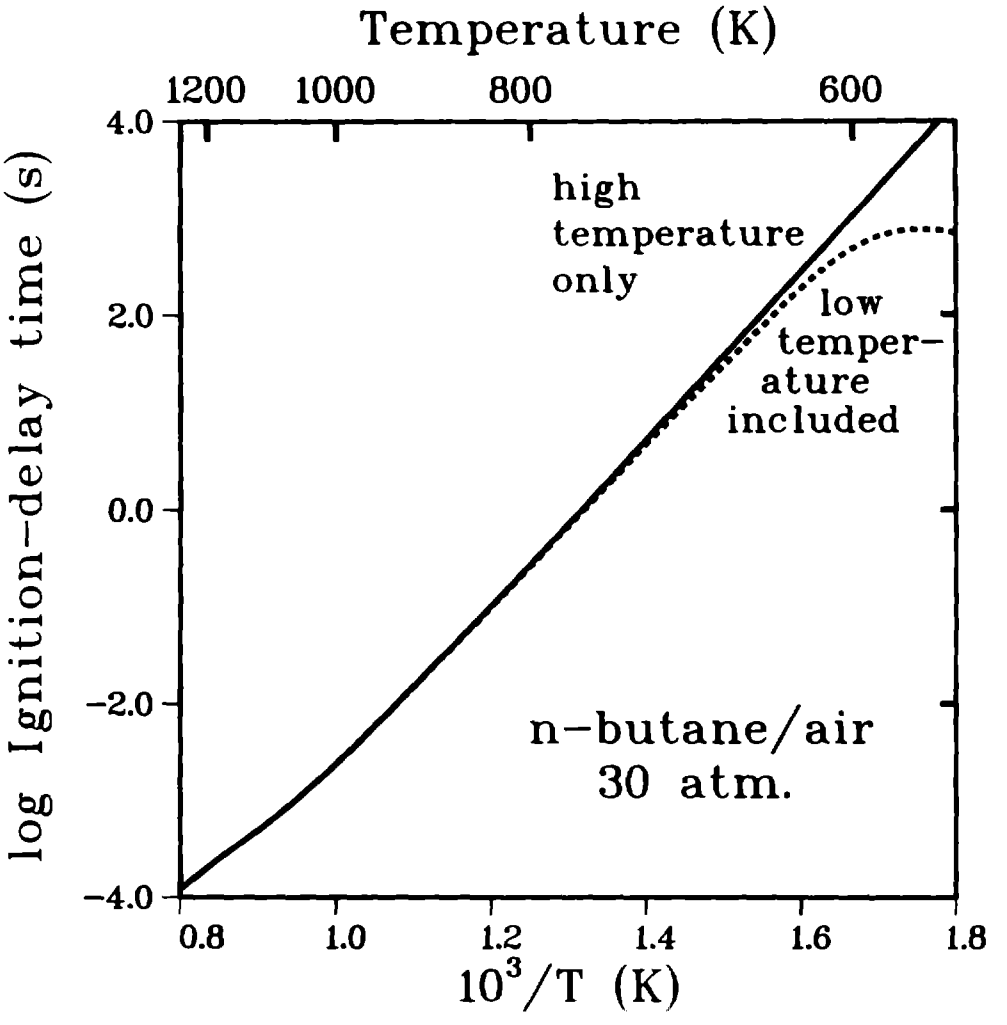

Figure 3. Autoignition times for stoichiometric, n-butane-air at constant volume and an initial pressure of 30 Atm. Chemical kinetic reaction mechanisms used: ——— Table I only, – – – both Table I and Table II.

CHEMICAL KINETICS

The chemical kinetic reactions for which the autoignition calculations show sensitivity are identified in this section. For stoichiometric n-butane-air in an end-gas combustion environment, the primary reactions consuming the fuel are:

$$C_4H_{10} + OH = C_4H_9 + H_2O \quad (182, 183)$$

$$C_4H_{10} + HO_2 = C_4H_9 + H_2O_2 \quad (194, 195)$$

$$C_4H_{10} + CH_3 = C_4H_9 + CH_4 \quad (186, 187)$$

$$C_4H_{10} + H = C_4H_9 + H_2 \quad (180, 181)$$

During the very early stages of fuel oxidation (about 0.7 ms ATDC), Reactions 194 and 195 are almost entirely responsible for fuel consumption. These reactions produce H_2O_2 which then decomposes

$$H_2O_2 + M = OH + OH + M \quad (13)$$

This reaction sequence is the primary chain branching path in the autoignition calculations. Fuel consumption, which occurs in the last 0.6 ms before autoignition (Fig. 1b), is particularly sensitive to the rates of this reaction path. A factor of two decrease in rates of Reactions 194 and 195 or 13 produces an approximately 25 percent increase in the fuel consumption time period (Table III).

The butyl radicals resulting from fuel consumption can either react with O_2 or thermally decompose:

$$C_4H_9 + O_2 = C_4H_8 + HO_2 \quad (200,204,205)$$

$$pC_4H_9 = C_2H_4 + C_2H_5 \quad (198)$$

$$sC_4H_9 = C_3H_6 + CH_3 \quad (203)$$

For the butyl radical sC_4H_9, the fraction that thermally decomposes

compared to that which reacts with oxygen is important. When it reacts with O_2 (Reaction 204 and 205), HO_2 is produced which can then react with the fuel and yield H_2O_2. The hydrogen peroxide rapidly decomposes (Reaction 13) into two hydroxyl radicals which can then react with the fuel by Reaction 182 and 183. This sequence tends to accelerate the autoignition process. However, if sC_4H_9 thermally decomposes (Reaction 203), the products C_3H_6 and CH_3 are produced which are relatively unreactive. This leads to a slowing of the overall fuel oxidation. These accelerating and inhibiting sequences illustrate the important role which HO_2 and H_2O_2 play in the autoignition process.

The radical-radical reaction

$$CH_3 + HO_2 = CH_3O + OH \qquad (38)$$

has a significant effect on autoignition times since it produces an OH radical and an additional H or HO_2 through

$$CH_3O + O_2 = CH_2O + HO_2 \qquad (46)$$

$$CH_3O + M = CH_2O + H + M \qquad (45)$$

Sensitivities for many reactions were determined and are given in Table III. To obtain these sensitivities, the reaction rate under consideration was multiplied by 2.0 or 0.5. The autoignition calculation of Fig. 1 was performed, and the autoignition time was compared to the original time. The ratio of the change in autoignition time to the reference fuel consumption period (0.6 ms) is presented in Table III.

ANTIKNOCKS

The current modeling calculations have shown that reactions involving HO_2 have a dominating role in autoignition at high pressures and moderately

Table III

Reaction rate sensitivity

Reaction	Percent change in fuel consumption period: 2 x rate	0.5 x rate
$C_4H_{10}+HO_2 = C_4H_9+H_2O_2$	-22	26
$H_2O_2+M = OH+OH+M$	-13	22
$CH_3+HO_2 = CH_3O+OH$	-21	43
$H+O_2 = OH+O$	- 8	6
$sC_4H_9+O_2 = C_4H_8+HO_2$	- 7	--
$sC_4H_9 = C_3H_6+CH_3$	8	--
$C_2H_5+O_2 = C_2H_4+HO_2$	- 4	--
$pC_4H_9+O_2 = 1C_4H_8+HO_2$	- 3	--
$C_4H_{10}+O_2 = C_4H_9+HO_2$	1	--
$H+O_2 = OH+O$	- 8	6
$C_4H_{10}+OH = pC_4H_9+H_2O$	- 3	--
$C_4H_{10}+OH = sC_4H_9+H_2O$	--	0[b]
$C_4H_{10}+OH = C_4H_9+H_2O$	- 1	--
$C_4H_{10}+H = pC_4H_9+H_2$	1	- 1
$C_4H_{10}+H = sC_4H_9+H_2$	2	- 1

-- Sensitivity calculation not performed.
b Sensitivity < 0.5 %

high temperatures ($20 < P < 30$ atm; $900 < T < 1300$ K). The most important of these are the fuel abstraction reactions which produce H_2O_2 which subsequently yields two OH radicals:

$$C_4H_{10} + HO_2 = C_4H_9 + H_2O_2 \qquad (182, 183)$$

$$H_2O_2 + M = OH + OH + M \qquad (13)$$

This is a chain branching path that accelerates autoignition. An antiknock might provide a terminating path that slows autoignition. An antiknock, A, could compete for HO_2 and/or H_2O_2

$$A + HO_2 \rightarrow B \qquad (I)$$

$$A + H_2O_2 \rightarrow C \qquad (II)$$

and produce relatively unreactive products B and C. If either Reaction I or II is sufficiently fast and the concentration of A sufficiently large, the autoignition process would be significantly inhibited. Steps I and II may actually be a more complicated process than indicated by the above, one-step reactions. A series of detailed reactions could occur whose overall effect is represented by I and II. Furthermore, HO_2 or H_2O_2 may not directly react with A but with a by-product or fragment of A.

CONCLUSIONS

An autoignition model using a high temperature reaction mechanism for n-butane predicted an autoignition time in close agreement with the measured time of knock in an actual engine. The inclusion of a low temperature reaction submechanism (Table II) had no effect on autoignition times. This result suggests that low temperature reaction paths such as those encountered in cool flames may not be important in affecting autoignition times at engine

conditions. The end-gas may spend too little time at low temperatures for these paths to have an effect.

The consumption of HO_2 and subsequent chain branching through H_2O_2 was identified as an important chemical kinetics path. This reaction sequence accelerates autoignition at temperatures and pressures relevant to engine knock. An antiknock that provides a competitive and terminating path for HO_2 or H_2O_2 would be an effective inhibitor of autoignition.

ACKNOWLEDGMENTS

The authors gratefully acknowledge Drs. Ray Smith and Bob Green of Sandia National Laboratories for many useful discussions and for the use of their data prior to its publication. Helpful discussions with Professor Nicholas P. Cernansky of Drexel University, Professor Frederick L. Dryer of Princeton University and Professor A. K. Oppenheim of University of California are very much appreciated. This work was performed under the auspices of the U. S. Department of Energy by the Lawrence Livermore National Laboratory under contract No. W-7405-ENG-48.

REFERENCES

Bahn, G.S. (1973). Approximate thermochemical tables for some C-H and C-H-O species. NASA report NASA-CR-2178.

Benson, S.W. (1982). Cool flames and oxidation: mechanism, themochemistry and kinetics. Oxidation Communications 3, 169.

Carrier, G., Fendell, F., Fink, S. and Feldman, P. (1983). Heat transfer as a determent of end-gas knock. Presented at the Western States Section of the Combustion Institute, Fall meeting.

Dale, J.D. and Oppenheim, A.K. (1982). A rationale for advances in the technology of I.C. engines. SAE paper No. 820047.

Downs, D., Walsh, A.D. and Wheeler, R.W. (1951). A study of the reactions that lead to "knock" in the spark-ignition engine. Philosophical Transactions of Royal Society of London, Series A 243, 463.

Green, R.M. and Smith, J.R. (1984). An experimental study of engine knock. To be presented at the Western States Section of the Combustion Institute, Spring Meeting.

Halstead, M.P., Kirsch, L.J. and Quinn, C.P. (1977). The autoignition of hydrocarbon fuels at high temperatures and pressures - fitting of a mathematical model. Combustion and Flame 30, 45.

JANAF Thermochemical Tables (1971). U. S. Government Printing Office, Washington, D.C.

Leppard, W.R. (1983). A detailed chemical kinetics simulation of engine knock. Submitted for publication.

Lund, C.M. (1978). HCT-a general computer program for calculating time-dependent phenomena involving one-dimensional hydrodynamics, transport, and detailed chemical kinetics. Lawrence Livermore National Laboratory report UCRL-52504.

Maly, R. and Ziegler, G. (1982). Thermal combustion modeling - theoretical and expermental investigation of the knocking process. SAE paper No. 820759.

Martinez, M.R., Miller, D.J., and Thommarson, R.L. (1974). Automated estimation of kinetic rate parameters and mechanisms of gas phase chemical reactions. NTIS AD-774304.

Natarajan, B. and Bracco, F.V. (1983). On modeling autoignition in spark-ignition engines. Submitted for publication.

Obert, E.F. (1973). Internal Combustion Engines and Air Pollution, Harper and Row, Publishers, Inc., New York, p 234-235.

Pitz, W. J. and Westbrook, C. K. (1983). Chemical kinetics of engine knock: preliminary results. Presented at The Western States Section of the Combustion Institute, Fall Meeting.

Pitz, W.J., Westbrook, C.K., Proscia, W.M., and Dryer, F.L. (1984). A comprehensive chemical kinetic reaction mechanism for the oxidation of n-butane. To be presented at the Twentieth (International) Symposium on Combustion, Ann Arbor, Michigan.

Smith, J. R., Green, R. M., Westbrook, C. K., and Pitz, W. J. (1984). An experimental and modeling study of engine knock. To be presented at the Twentieth (International) Symposium on Combustion, Ann Arbor, Michigan.

Westbrook, C.K. and Dryer, F.L. (1983). Chemical kinetics modeling of hydrocarbon combustion. To be published in Progress in Energy and Combustion Science.

Westbrook, C. K. and Pitz, W. J. (1984). A comprehensive chemical kinetic reaction mechanism for oxidation and pyrolysis of propane and propene. Combustion Science and Technology 37, 117.